

ACCEPTED MANUSCRIPT

# Modelling the cerebral haemodynamic response in the physiological range of PaCO<sub>2</sub>

To cite this article before publication: Jatinder Singh Minhas *et al* 2018 *Physiol. Meas.* in press <https://doi.org/10.1088/1361-6579/aac76b>

## Manuscript version: Accepted Manuscript

Accepted Manuscript is “the version of the article accepted for publication including all changes made as a result of the peer review process, and which may also include the addition to the article by IOP Publishing of a header, an article ID, a cover sheet and/or an ‘Accepted Manuscript’ watermark, but excluding any other editing, typesetting or other changes made by IOP Publishing and/or its licensors”

This Accepted Manuscript is © 2018 Institute of Physics and Engineering in Medicine.

During the embargo period (the 12 month period from the publication of the Version of Record of this article), the Accepted Manuscript is fully protected by copyright and cannot be reused or reposted elsewhere.

As the Version of Record of this article is going to be / has been published on a subscription basis, this Accepted Manuscript is available for reuse under a CC BY-NC-ND 3.0 licence after the 12 month embargo period.

After the embargo period, everyone is permitted to use copy and redistribute this article for non-commercial purposes only, provided that they adhere to all the terms of the licence <https://creativecommons.org/licenses/by-nc-nd/3.0>

Although reasonable endeavours have been taken to obtain all necessary permissions from third parties to include their copyrighted content within this article, their full citation and copyright line may not be present in this Accepted Manuscript version. Before using any content from this article, please refer to the Version of Record on IOPscience once published for full citation and copyright details, as permissions will likely be required. All third party content is fully copyright protected, unless specifically stated otherwise in the figure caption in the Version of Record.

View the [article online](#) for updates and enhancements.

1  
2  
3 1  
4  
5 2  
6  
7 3  
8  
9 4  
10  
11 5  
12  
13 6  
14  
15 7  
16  
17 8  
18 9  
19  
20 10  
21 11  
22 12  
23  
24 13  
25 14  
26  
27 15  
28  
29 16  
30 17  
31  
32  
33  
34  
35  
36  
37  
38  
39  
40  
41  
42  
43  
44  
45  
46  
47  
48  
49  
50  
51  
52  
53  
54  
55  
56  
57  
58  
59  
60

## **Modelling the cerebral haemodynamic response in the physiological range of PaCO<sub>2</sub>**

**Minhas JS<sup>1</sup>, Panerai RB<sup>1,2</sup>, Robinson TG<sup>1,2</sup>**

<sup>1</sup>Cerebral Haemodynamics in Ageing and Stroke Medicine (CHIASM) Research Group, Department of Cardiovascular Sciences, University of Leicester, Leicester, United Kingdom.

<sup>2</sup>National Institute for Health Research Leicester Biomedical Research Centre, University of Leicester, Leicester, United Kingdom

Corresponding Author: Dr Jatinder S. Minhas, [jm591@le.ac.uk](mailto:jm591@le.ac.uk), Level 2, Sir Robert Kilpatrick Clinical Sciences Building, Leicester Royal Infirmary, Leicester, LE2 7LX, +44 116 252 5814.

**Running Title: Cerebral haemodynamics in the physiological range of PaCO<sub>2</sub>**

Keywords: blood pressure, carbon dioxide, haemodynamics

1  
2  
3 18 **Abbreviations list**  
4

5 19  
6  
7 20 ARI Autoregulation index  
8  
9 21 BP Blood pressure  
10  
11 22 CA Cerebral autoregulation  
12  
13 23 CBFV Cerebral blood flow velocity  
14  
15 24 CO<sub>2</sub> Carbon dioxide  
16  
17 25 CrCP Critical closing pressure  
18  
19 26 CVMR Cerebral vasomotor reactivity  
20  
21 27 dCA Dynamic cerebral autoregulation  
22  
23 28 ECG Electrocardiogram  
24  
25 29 EtCO<sub>2</sub> End-tidal CO<sub>2</sub>  
26  
27 30 HR Heart rate  
28  
29 31 MABP Mean arterial blood pressure  
30  
31 32 MCA Middle cerebral artery  
32  
33 33 PaCO<sub>2</sub> Partial pressure carbon dioxide  
34  
35 34 RAP Resistance-area product  
36  
37 35 SD Standard deviation  
38  
39 36 TCD Transcranial Doppler  
40  
41 37 TFA Transfer function analysis  
42  
43  
44  
45  
46  
47  
48  
49  
50  
51  
52  
53  
54  
55  
56  
57  
58  
59  
60

**Abstract****Objective**

Arterial CO<sub>2</sub> (PaCO<sub>2</sub>) has a strong effect on cerebral blood flow (CBF), but its influence on CBF regulatory mechanisms and circulatory systemic variables has not been fully described over the entire physiological range of PaCO<sub>2</sub>.

**Approach**

CBF velocity (CBFV, transcranial Doppler), blood pressure (BP, Finometer) and end-tidal CO<sub>2</sub> (EtCO<sub>2</sub>, capnography) were measured in 45 healthy volunteers (19 male, mean age 37.5 years, range 21-71) at baseline, and in response to hypo- (-5mm Hg and -10mm Hg below baseline) and hypercapnia (5% and 8% CO<sub>2</sub>), applied in random order.

**Main Results**

CBFV, cerebral dynamic autoregulation index (ARI), heart rate (HR), arterial blood pressure (ABP), critical closing pressure (CrCP) and resistance-area product (RAP) changed significantly (all  $p < 0.0001$ ) for hypo- and hyper-capnia. These parameters were shown to follow a logistic curve relationship representing a 'dose-response' curve for the effects of PaCO<sub>2</sub> on the cerebral and systemic circulations. The four logistic model parameters describing each 'dose-response' curve were specific to each of the modelled variables (ANOVA  $p < 0.0001$ ).

**Significance**

The ability to model the CBFV, ARI, HR, ABP, CrCP and RAP dependency of PaCO<sub>2</sub> over its entire physiological range is a powerful tool for physiological and clinical studies, including the need to perform adjustments in disease populations with differing values of baseline PaCO<sub>2</sub>.

## 60 Introduction

61  
62 Cerebral autoregulation (CA) is usually defined as the tendency of cerebral blood flow (CBF)  
63 to remain approximately constant despite changes in blood pressure (BP) within the range 50  
64 to 170 mmHg (Lassen 1959, Paulson *et al* 1990). However, outside these limits, CA  
65 becomes passive and CBF follows changes in response to BP. Importantly, this classical  
66 relationship, usually referred to as ‘static’ CA, has been challenged and ultimately the  
67 physiological properties of CA remain largely inconclusive (Willie *et al* 2014, Tzeng,  
68 Ainslie 2014, Tymko, Ainslie 2017). Dynamic CA (dCA) can be estimated from the transient  
69 response of CBF to rapid changes in BP (Aaslid *et al* 1989) and this has been the preferred  
70 approach for the assessment of CA in human physiological and clinical studies (Reivick 1964,  
71 Ogoh *et al* 2010, Battisti-Charbonney *et al* 2011). Understanding the dCA response to  
72 physiological manoeuvres, such as exercise and changes in respiratory patterns, has often been  
73 confounded by simultaneous changes in the arterial partial pressure of carbon dioxide (PaCO<sub>2</sub>)  
74 (Ogoh *et al* 2008, Dineen *et al* 2010). Hypercapnia leads to vasodilation of cerebral vessels  
75 (Markwalder *et al* 1984) and overall causes deterioration in CA (Aaslid *et al* 1989).  
76 Conversely, hypocapnia has a vasoconstrictive effect, improving CA (Aaslid *et al* 1989, Ogoh  
77 *et al* 2008, Ainslie *et al* 2008, Dineen *et al* 2010). Indeed, experimental work has suggested  
78 hypercapnia can be used to emulate a state of impaired dCA (Maggio *et al* 2013). Although  
79 these effects of PaCO<sub>2</sub> changes on CBF and dCA are widely accepted qualitatively, there is a  
80 need for a comprehensive quantitative model covering the entire physiological range of PaCO<sub>2</sub>,  
81 to allow further refinements in the data analysis of physiological and clinical cerebrovascular  
82 studies. This is crucial for cerebral haemodynamic parameters as well as systemic  
83 haemodynamic parameters as these are often considered significant confounders when  
84 assessing blood flow during physiologically vulnerable states like altitude, extremes of exercise  
85 and acute neurological emergencies.

86  
87 Changes in PaCO<sub>2</sub> induced by transient breath-by-breath adjustment demonstrates non-linear  
88 effects on CBF (Poulin *et al* 1996, Ide *et al* 2003, Claassen *et al* 2007, Ainslie *et al* 2008,  
89 Duffin *et al* 2017). Amongst different potential non-linear models, the logistic function has  
90 been shown to provide a realistic description of the cerebral blood flow velocity (CBFV),  
91 responding to changes in PaCO<sub>2</sub> (Claassen *et al* 2007). Logistic models have also proved  
92 successful to describe the effects of PaCO<sub>2</sub> on cerebrovascular conductance index (CVCi)  
93 (Claassen *et al* 2007) and cerebrovascular resistance (Duffin *et al* 2017).

94  
95 Current understanding of vascular physiology principles has led to models adopting the  
96 principle that vascular bed resistance-CO<sub>2</sub> response relationships are sigmoidal (Duffin *et al*  
97 2017). Although logistic modelling has been applied to parameters like branch pressure or  
98 resistance, there is a clear clinical importance in developing such models in health and  
99 pathological states to help understand variations in cerebrovascular CO<sub>2</sub> responsiveness.

100  
101 We used a wide range of PaCO<sub>2</sub> within a multi-step protocol to test for the first time the  
102 hypotheses that i) a commonly used index of dCA, the autoregulation index (ARI) shows a  
103 dependence on PaCO<sub>2</sub> following a logistic non-linear model, similar to that described for  
104 CBFV; and ii) key cerebral haemodynamic parameters including ABP, heart rate (HR), critical  
105 closing pressure (CrCP) and resistance-area product (RAP) can also have their dependence on  
106 PaCO<sub>2</sub> described by a logistic non-linear model.

107

## 108 **Methods**

### 109 **Subjects and measurements**

110 The study was conducted in accordance with the Declaration of Helsinki (2000). Ethical  
111 approval was obtained from the University of Leicester Ethics Committee (Reference: jm591-  
112 c033). Healthy volunteers were recruited from University departmental staff, students and their  
113 relatives. Participants aged above 18 years were included. Exclusion criteria were physical  
114 disease in the upper limb, poor insonation of both temporal bone windows and any significant  
115 history of cardiovascular, neurological or respiratory disease. All participants provided written,  
116 informed consent.

117 The research was undertaken in the University of Leicester's *Cerebral Haemodynamics in*  
118 *Ageing and Stroke Medicine* research laboratory, maintained at a constant ambient temperature  
119 of approximately 24°C and free of distraction. For the purposes of the study, participants were  
120 asked to refrain from caffeine, alcohol and nicotine in the 12-hour period prior to measurements  
121 being undertaken. Beat-to-beat BP was recorded continuously using the Finometer® device  
122 (FMS, Finapres Measurement Systems, Arnhem, Netherlands), which was attached to the  
123 middle finger of the left hand. The servo-correcting mechanism of the Finometer® was  
124 switched on and then off prior to measurements. The hand bearing the finger cuff was at the  
125 level of the heart to negate any hydrostatic pressure artefact. HR was recorded using a standard

1  
2  
3 126 3-lead electrocardiogram (ECG). EtCO<sub>2</sub> was measured throughout the initial resting baseline  
4  
5 127 and hypercapnic phase using a face-mask connected to a capnograph (Capnograph Plus).  
6  
7 128 During the second baseline and hypocapnic phase EtCO<sub>2</sub> was measured via nasal prongs (Salter  
8  
9 129 Labs). Bilateral insonation of the middle cerebral arteries (MCAs) was performed using  
10  
11 130 transcranial Doppler (TCD) ultrasound (Viasys Companion III; Viasys Healthcare) with a  
12  
13 131 2MHz probe. This probe was secured in place with a head-frame that was adjusted to ensure  
14  
15 132 comfort at the outset. The MCAs were identified according to two main characteristics: signal  
16  
17 133 depth and velocities.

### 18 134 **Experimental protocol**

19  
20 135 All measurements were conducted at a single visit. Prior randomization of the order of hypo-  
21  
22 136 and hypercapnia was conducted using a random number generator. An initial period of 15  
23  
24 137 minutes of stabilization preceded a 5-minute baseline recording supine at rest. This was  
25  
26 138 followed by inspiring CO<sub>2</sub> in air, constantly ('fixed inspiration') for a minimum of 90 s (ideally  
27  
28 139 120 s) with either 5% CO<sub>2</sub> or 8% CO<sub>2</sub> in air (dependent on randomization). Each gas inspiration  
29  
30 140 episode was preceded by a 90 s recording to achieve physiological stability before and  
31  
32 141 immediately after the hypercapnia study period. After a further period of 5 min of stabilization,  
33  
34 142 participants performed a 5 min baseline recording and then were asked to hyperventilate in  
35  
36 143 random order, as previously described, at different respiratory rates to produce incremental  
37  
38 144 reductions in EtCO<sub>2</sub> of 5mmHg and 10mmHg less than normocapnia for that individual.  
39  
40 145 Hyperventilation was sustained for a minimum period of 90 s, or a maximum of 120 s. For  
41  
42 146 hyperventilation, participants were asked to breathe with a metronome (KORG Metronome  
43  
44 147 MA-30) creating a respiratory rate of at least 5 breaths per minute above their resting rate for  
45  
46 148 at least 90 s without specific control of amplitude of breathing. Two-minute washout periods  
47  
48 149 of normal respiration were allowed between successive measurements. Each incremental  
49  
50 150 reduction in EtCO<sub>2</sub> was repeated on two occasions during the same session. Measurements  
51  
52 151 were continuously recorded at a rate of 500 samples/s in the PHYSIDAS data acquisition  
53  
54 152 system (Department of Medical Physics, University Hospitals of Leicester). Systolic and  
55  
56 153 diastolic brachial BP readings (OMRON Model 705IT) were performed at each stage of the  
57  
58 154 protocol (normocapnia, hypercapnia and hypocapnia) with a minimum of 3 recordings per  
59  
60 155 individual. These values were then used to calibrate the Finometer recordings.

### 57 156 **Data Analysis**

1  
2  
3 157 Data collected corresponded to six individual files for each participant: 2 at baseline, 2  
4 158 hypercapnic and 2 hypocapnic. First, data were inspected visually and calibrated to recorded  
5 159 systolic and diastolic OMRON BP. Narrow spikes (<100ms) were removed using linear  
6 160 interpolation and the CBFV recording was then passed through a median filter. All signals were  
7 161 then low pass filtered with a zero-phase Butterworth filter with cut-off frequency of 20Hz.  
8 162 Automatic detection of the QRS complex of the ECG, to mark the R-R interval was used, but  
9 163 also visual inspection was undertaken with and manual correction whenever necessary. This  
10 164 allowed mean ABP, HR, EtCO<sub>2</sub> and mean CBFV to be calculated for each cardiac cycle. CrCP  
11 165 and RAP were estimated using the first harmonic method (Panerai 2003). Randomization was  
12 166 not disclosed until data collection was completed.

13 167 Given the non-stationary influence of PaCO<sub>2</sub> on dCA, ARI, proposed by Tiecks *et al* (Tiecks  
14 168 *et al* 1995) was calculated as a function of time (ARIt), using a moving-window, autoregressive  
15 169 moving average (ARMA) model, that follows the same structure as the second-order  
16 170 differential equation proposed by Tiecks *et al* (1995) as described previously (Dineen *et al*  
17 171 2010). In short, with V(t) representing beat-to-beat changes in CBFV and dP(t) corresponding  
18 172 changes in BP, normalised by CrCP (Tiecks *et al* 1995), the two quantities are linked by:

$$\hat{V}(t) = 1 + dP(t) - K \times x_2(t) \quad [1]$$

19 173 where K represents a gain parameter in the second order equation, and x<sub>2</sub>(t) is a state variable obtained  
20 174 from the following state equation system representing a second-order equation:

$$x_1(t) = x_1(t-1) + \frac{dP(t-1) - x_2(t-1)}{f \times T} \quad [2]$$

21 175

$$x_2(t) = x_2(t-1) + \frac{x_1(t-1) - 2 \times D \times x_2(t-1)}{f \times T} \quad [3]$$

22 176

23 177 where parameters T and D correspond to the damping and time-constant terms of a second  
24 178 order model, and f is the inverse of the sampling frequency (Tiecks *et al* 1995).

25 179 From these equations, it is possible to demonstrate (Dineen *et al* 2010) that eq. 1 can be  
26 180 expressed as a discrete ARMA model, that is:

$$v(n) = ap(n) + b[p(n-1) - v(n-1)] + c[p(n-2) - v(n-2)] \quad [4]$$

where  $v(n)$  and  $p(n)$  are discrete samples of  $V(t)$  and  $P(t)$ , respectively, and the coefficients  $a$ ,  $b$  and  $c$  are directly related to the original parameters  $K$ ,  $D$ ,  $T$  above.

The ARMA model was applied for a 60 s time moving window using BP as input and CBFV as output. Using the model coefficients ( $a$ ,  $b$ ,  $c$ ), the CBFV response to a step change in BP was obtained and the corresponding value of ARI was estimated by fitting one of the 10 CBFV step responses proposed by Tiecks *et al* (Tiecks *et al* 1995). The complete time-series of ARI values for each recording was obtained by moving the time-window at 0.6s intervals. Values of  $ARI_{t=0}$  represent absence of autoregulation, whilst  $ARI_{t=9}$  corresponds to the most efficient CA that can be observed. The ARI time-series was computed for each subject separately for left and right hemispheres for each recording.

### 192 *Logistic Model*

193 Following the logistic model for the effects of  $CO_2$  on CBFV (Claassen *et al* 2007), a similar  
194 model was adopted, and was also extended to test the feasibility of using the logistic  
195 relationship to express the influence of  $CO_2$  on dCA and other systemic and cerebrovascular  
196 parameters. The logistic model adopted is given by:

$$197 \quad y = y_{max} + \frac{y_{min} - y_{max}}{1 + e^{k(x-x_0)}} \quad [5]$$

198 where  $y$  can represent either mean CBFV, ABP, HR, CrCP, RAP or ARI.  $x$  is the  $EtCO_2$  level  
199 and  $k$  is the exponential coefficient. Fitting the model allows estimation of its four parameters,  
200 namely  $y_{max}$ ,  $y_{min}$ ,  $k$  and  $x_0$  (Figure 1).

201 Model parameters were obtained by combining least squares with a recursive bootstrap  
202 technique to remove outliers. After estimation of ARI for each of the six different recordings  
203 (two each, for baseline, hyperventilation, and  $CO_2$  breathing), each recording was divided into  
204 four segments and the mean CBFV, ABP, HR, CrCP, RAP, ARI and  $EtCO_2$  of each segment  
205 was used to fit equation 1 using 24 sample values (4 segments for 6 recordings) to express the  
206 effects of  $PaCO_2$  on these six different parameters. After each stage of error minimization by  
207 least squares, the largest outlier was identified and the process repeated for a maximum of eight  
208 potential outliers. The minimum square error (MSE) and the estimated parameters at each stage  
209 were listed and the number of outliers to be removed was chosen under visual inspection, to  
210 select model parameters that were stable and a region of MSE that was not critically dependent

1  
2  
3 211 on the number of outliers removed. In general, the final number of outliers removed was eight  
4 212 or less. The advantages and limitations of this new approach will be discussed later.

5  
6  
7 213 **Statistical Analysis**  
8

9  
10 214 The study protocol was tested for differences in each level of CO<sub>2</sub> using one-way ANOVA.  
11 215 Data normality was assessed with the Kolmogorov-Smirnov test. Baseline measurements were  
12 216 assessed for differences between values derived for right and left hemispheres using a paired  
13 217 Student's t-test. These were averaged when no significant differences were found. Repeated  
14 218 measures ANOVA was used to assess for differences between model parameter values for each  
15 219 haemodynamic parameter group.  
16  
17  
18  
19  
20  
21  
22  
23  
24  
25  
26  
27  
28  
29  
30  
31  
32  
33  
34  
35  
36  
37  
38  
39  
40  
41  
42  
43  
44  
45  
46  
47  
48  
49  
50  
51  
52  
53  
54  
55  
56  
57  
58  
59  
60

## 220 **Results**

221 Forty-five subjects (19 male) of mean age 37.5 years (range 21 to 71) were included in the  
222 analyses. None of the subjects were smokers or had diabetes.

223 Differences between recordings from the right and left MCA were not significant for any of  
224 the bilateral parameters considered, averaged values for the two sides were used in all  
225 subsequent analyses. Baseline cerebral haemodynamic parameters are presented in Table 1.

### 226 *Effect of hypo- and hypercapnia on cerebral haemodynamics*

227 Highly significant differences in EtCO<sub>2</sub> resulted from breathing CO<sub>2</sub> in air and hyperventilation  
228 (ANOVA  $p < 0.0001$ ) leading to EtCO<sub>2</sub> values of 46.5 (3.7) mmHg (8% CO<sub>2</sub>), 42.7 (3.5) mmHg  
229 (5% CO<sub>2</sub>), 37.8 (3.1) mmHg (baseline), 30.1 (5.7) (-5 mmHg hyperventilation) and 28.5 (5.7)  
230 mmHg (-10 mmHg hyperventilation).

231 A representative recording is presented in Figure 2, showing the temporal patterns of changes  
232 in ABP, CBFV and EtCO<sub>2</sub> observed during normo-, hypo- and hypercapnia. For the same  
233 subject, Figure 3 shows the corresponding fitting of the data to the logistic model for both  
234 CBFV and ARI. Similar models were obtained for ABP, HR, CrCP and RAP.

235 Population values of model parameters are given in Table 2, with corresponding population  
236 average logistic curves represented in Figure 4. In all cases the dependence on EtCO<sub>2</sub> reflects  
237 the expected physiological effects of PaCO<sub>2</sub> on each of the parameters modelled as will be  
238 discussed below.

239 The model parameters  $k$  and  $x_0$  were different when assessed for between group differences for  
240 all haemodynamic parameters. The model parameter  $k$  was different between haemodynamic  
241 parameter groups ( $p < 0.0001$ ) with HR demonstrating the largest value (SD) of  $1.00 \text{ mmHg}^{-1}$   
242 (0.8). The model parameter  $x_0$  was different between haemodynamic parameter groups  
243 ( $p = 0.004$ ) with CrCP demonstrating the largest value (SD) of 38.4 mmHg (4.3). There were no  
244 outliers removed from CBFV, ARI, CrCP or RAP analyses. Eight outliers or less were removed  
245 for ABP (Median 6, IQR 4-7) and HR (Median 6, IQR 4-7).

246

## 247 Discussion

### 248 *Main findings*

249 To our knowledge this is the largest study to date to describe the effects of PaCO<sub>2</sub> on CBFV,  
250 ABP, HR, CrCP and RAP, and the first to demonstrate a logistic model relationship between  
251 ARI and EtCO<sub>2</sub>, across a wide physiological range.

### 253 *Effects of carbon dioxide on cerebral autoregulation*

254 For many pharmacological agents, regression of the stimulus on organ response is non-linear  
255 (Kenakin 1997). The dependence of CBF, usually estimated from non-invasive measurements  
256 of CBFV with TCD ultrasonography, on PaCO<sub>2</sub> has been previously quantified by exponential  
257 (Markwalder *et al* 1984) or logistic curves, using EtCO<sub>2</sub> as the independent variable (Claassen  
258 *et al* 2007). The demonstration that ARI, a widely used index of dCA, decreases as EtCO<sub>2</sub> rises,  
259 also following a logistic curve, is of considerable relevance. Above all, the possibility of using  
260 the 4-parameter logistic curve to provide a complete representation of CA dependence on  
261 PaCO<sub>2</sub> (Figures 2 and 3) can be seen as an entirely new paradigm for the simultaneous  
262 assessment of dCA and CO<sub>2</sub> reactivity in individuals or populations. This new approach could  
263 provide a much more robust ‘fingerprint’ to characterise CBF regulatory mechanisms, than the  
264 use of separate indices that are plagued by issues of reliability due to the interaction of multiple  
265 co-factors and poor reproducibility. Since the logistic curve is derived from six different 5-min  
266 recordings, it provides a much broader assessment of the response of CBF regulatory  
267 mechanisms. The implications of this new approach for clinical studies will be discussed  
268 below.

269  
270 Previous studies have mainly concentrated on the effects of PaCO<sub>2</sub> on CBF or CBFV, reporting  
271 non-linear relationships including sigmoidal curves as in our case (Claassen *et al* 2007, Battisti-  
272 Charbonney *et al* 2011). On the other hand, Ainslie *et al* (Ainslie *et al* 2008) reported on the  
273 effects of PaCO<sub>2</sub> on TFA measures of dynamic CO<sub>2</sub> using a protocol similar to ours, that is two  
274 hypercapnic and two hypocapnic levels. Nevertheless, parameters of gain and phase, often  
275 associated with dCA performance did not show a consistent relationship with EtCO<sub>2</sub> as we  
276 found for ARI. One possible explanation is the reduced sensitivity of using separate measures  
277 of gain and phase, and the fact that the ARI incorporates all the information obtained with TFA  
278 thus providing a more robust measure of dCA (Claassen *et al* 2016). Although other studies  
279 have described changes in dCA with different levels of PaCO<sub>2</sub>, direct comparisons are hindered

1  
2  
3 280 by the use of different protocols (e.g. thigh cuffs instead of spontaneous fluctuations in BP), or  
4  
5 281 only 2-point comparisons (usually normocapnia to hypercapnia), which does not allow for  
6  
7 282 identification of the nature of the entire dependence of dCA on EtCO<sub>2</sub> (Aaslid *et al* 1989,  
8  
9 283 Panerai *et al* 1999, Dineen *et al* 2010, Ogoh *et al* 2010, Maggio *et al* 2013).

10 284  
11  
12 285 Accordingly, it is important to determine that any differences in cerebral haemodynamic  
13  
14 286 responses that are observed between different physiological conditions or between healthy and  
15  
16 287 disease states are not confounded by differences in PaCO<sub>2</sub> (Willie *et al* 2012, Battisti-  
17  
18 288 Charbonney, Fisher & Duffin 2011). For example in a healthy control population, Ogoh *et al*  
19  
20 289 (Ogoh *et al* 2010) demonstrated that hypoxia disrupts dCA, but hypocapnia augments the dCA  
21  
22 290 response. Furthermore, in our own previous work in an acute ischemic stroke population  
23  
24 291 (Salinet *et al* 2015) measures of cerebrovascular reactivity and neurovascular coupling were  
25  
26 292 impaired compared to controls, though dCA was not. However, baseline hypocapnia in the  
27  
28 293 stroke population may have confounded the effect size. Therefore, there is significant merit in  
29  
30 294 describing the complete relationship between dCA across a physiological range of PaCO<sub>2</sub>,  
31  
32 295 including both hypo- and hyper-capnia that could be used to establish comparisons between  
33  
34 296 individuals with different levels of PaCO<sub>2</sub>.

35 297  
36 298 Currently, there are no studies that have demonstrated PaCO<sub>2</sub> stimulus-response curves for an  
37  
38 299 extended set of variables like CBFV, ARI, ABP, HR, CrCP, RAP, ARIt. Other associated work  
39  
40 300 has demonstrated a sigmoidal relationship between PaCO<sub>2</sub> and vascular resistance using BOLD  
41  
42 301 as a surrogate for CBF as well as speed of response to hypercapnic stimulus (Poublanc *et al*  
43  
44 302 2015, Duffin *et al* 2017). The ‘model branch pressure’ reported by Duffin *et al* (Duffin *et al*  
45  
46 303 2017) also has the potential to be represented by a logistic model as demonstrated within this  
47  
48 304 study. With reference to RAP and CrCP, previous work (Panerai 2003, Ainslie *et al* 2008,  
49  
50 305 Grune *et al* 2015) has shown RAP and CrCP decrease with PaCO<sub>2</sub> with this particular study  
51  
52 306 providing no data on associated HR changes though highlighting a relatively static ABP (Grune  
53  
54 307 *et al* 2015). Prior work has shown that RAP increases significantly with hypocapnia with  
55  
56 308 similar findings as in our study population (McCulloch, Turner 2009).

57 309  
58 310 Hypercapnia leads to vasodilation of the cerebral microcirculation, whilst hypocapnia has the  
59  
60 311 opposite effect. These major effects explain the directional changes reflected by the logistic  
312 curves of CBFV, ARI, CrCP and RAP (Figure 3). On the other hand, the increase in BP with  
313 EtCO<sub>2</sub> has been explained by the increased sympathetic activity induced by hypercapnia

1  
2  
3 314 (Claassen *et al* 2007, Ainslie *et al* 2008, Grune *et al* 2015). The small reduction in HR across  
4  
5 315 the range of EtCO<sub>2</sub> values represented in Figure 3 though, might be more controversial. Ainslie  
6  
7 316 *et al* (Ainslie *et al* 2008) reported HR following a U-shaped curve when EtCO<sub>2</sub> changed from  
8  
9 317 hypocapnia to hypercapnia. As in our case, their mean BP increased with hypercapnia. With  
10  
11 318 an intact baroreceptor reflex, this increase in BP would be expected to lead to a reduction in  
12  
13 319 HR, as in our case, but it is possible that in their study, increased sympathetic activity in  
14  
15 320 hypercapnia dominated over the reduction in HR induced by the baroreflex. Further work is  
16  
17 321 needed to improve our understanding of the effects of PaCO<sub>2</sub> on heart rate.  
18

19 322  
20 323 We provide a novel evolution from original logistic relationship studies (Markwalder *et al*  
21  
22 324 1984, Claassen *et al* 2007). This study provides a wider range of PaCO<sub>2</sub> and more participants  
23  
24 325 than Markwalder *et al* (Markwalder *et al* 1984) originally used for corrective velocity  
25  
26 326 experiments on PaCO<sub>2</sub> values in 31 individuals and the Claassen *et al* (Claassen *et al* 2007)  
27  
28 327 study demonstrating modified logistic function of CBFV to transient changes in CO<sub>2</sub> in 10  
29  
30 328 subjects.

### 31 329 32 330 *Clinical perspectives*

33 331 An important outcome from this study is the potential to improve comparability of dCA  
34  
35 332 estimates for different patients with different PaCO<sub>2</sub> readings. The clinical necessity of this  
36  
37 333 previous limitation was demonstrated by Salinet *et al* (2015) who examined the effects of  
38  
39 334 cerebral ischemia on neurovascular coupling. They found no difference between groups  
40  
41 335 (patients vs. controls  $p=0.07$ ). They noted PaCO<sub>2</sub> levels were lower in the stroke population,  
42  
43 336 and concluded that if both groups were normalized to the same PaCO<sub>2</sub>, then CA would be  
44  
45 337 significantly impaired in the stroke group. This study provides a meaningful opportunity to  
46  
47 338 consider the extent to which “corrections” could be applied to healthy and potentially diseased  
48  
49 339 populations on the basis of the “dose-response” nature of EtCO<sub>2</sub> and dCA. Our study also  
50  
51 340 provides an example of how it would be possible to progress towards CO<sub>2</sub>-adjusted estimates  
52  
53 341 of ARI in future work. For this purpose, further studies involving larger number of individuals  
54  
55 342 are needed to assess the effects of sex, ethnicity and other potential co-factors. This would  
56  
57 343 provide an evolution from the standard CO<sub>2</sub> reactivity test (based on only two arbitrary points  
58  
59 344 taken from the entire curve). Finally, the reproducibility of such a marker in patient populations  
60  
345 does require validation, particularly as extremes of physiological variability have been shown  
346  
347 346 to alter reproducibility (Minhas *et al* 2016). However, previous studies in stroke patient  
populations (Salinet *et al* 2015) have shown less extreme variation in EtCO<sub>2</sub> values and hence

1  
2  
3 348 ARI (i.e. a trend towards hypocapnia). Instead of simply comparing values of ARI at single  
4  
5 349 operating points, determined by stable PaCO<sub>2</sub> values, the approach we are proposing, of  
6  
7 350 comparing the entire ARI curve as a function of EtCO<sub>2</sub> (Figure 3) might provide a much more  
8  
9 351 robust and general approach.

10 352

11 353 *Limitations of the study*

12 354 Several potential limitations must be considered in this study. First, with reference to TCD  
13 355 studies, changes in CBF can be accurately expressed by CBFV, as long as the diameter of the  
14 356 MCA remains constant. This assumption is usually acceptable at normocapnia or mild  
15 357 hypercapnia, but at moderate levels of hypercapnia, as we achieved in our subjects, it is likely  
16 358 that CBFV underestimated CBF, with hypocapnia leading to overestimation (Coverdale *et al*  
17 359 2014, Verbree *et al* 2014). Nevertheless, estimates of ARI (and TFA phase) are independent  
18 360 of the amplitude of CBFV and hence would not be distorted by MCA dilation. However, studies  
19 361 have shown cerebrovascular resistance to be an independent factor to PaCO<sub>2</sub> in altering  
20 362 pressure-flow dynamics and further studies are needed to assess this (Smirl *et al* 2014).  
21 363 Secondly, based on previous studies (Ogoh *et al* 2010, Panerai *et al* 1999) we have used a  
22 364 maximum of 8% CO<sub>2</sub> in air. Higher levels of CO<sub>2</sub> in air, for example 10%, could also be  
23 365 considered in future pilot studies to determine if the tail end of the ARI logistic curve (Figures  
24 366 2 & 3) can be reduced even further. Informed by previous work (Ainslie *et al* 2008), a washout  
25 367 period of 2 min. was adopted as standard for each individual. It remains unclear though,  
26 368 whether cerebral perfusion baselines were re-established in all individuals following  
27 369 hyperventilation. The randomisation procedure for hypocapnia may have led to an  
28 370 overestimation of dCA at the -5mmHg level if the individual was randomised to have the -10  
29 371 mmHg as the previous manoeuvre, as it proved difficult in some instances to fully establish a  
30 372 baseline due to the significant change in CBFV. Furthermore, some individuals found the 60  
31 373 to 120 s period during inhalation of the 8% CO<sub>2</sub> gas difficult and therefore the likelihood of  
32 374 mask leakage was more apparent due to increased anxiety and movement.

33 375

34 376 Thirdly, the use of a logistic curve model to represent the effects of PaCO<sub>2</sub> on CBFV, ABP,  
35 377 HR, CrCP, RAP and ARI should be regarded as a convenient and simplistic approximation to  
36 378 the true mathematical relationships, likely to be distinct for each of the dependent variables  
37 379 considered. The logistic model takes into account the expected behaviour and limited variation  
38 380 of physiological variables, thus showing gradual saturation at both extremes of PaCO<sub>2</sub>.  
39 381 Moreover, the fact that each curve is defined by four parameters (eq. 1) provides simplicity, on

1  
2  
3 382 one hand, but adequate flexibility on the other. Therefore, if for example, the relationship  
4  
5 383 tended to be more linear, this would be expressed by lower values of the parameter  $k$  (eq. 1).  
6  
7 384 Finally, the relatively low values of MSE obtained in each case (Table 1), also demonstrate the  
8  
9 385 appropriateness of using logistic curve models to describe the effects of  $\text{PaCO}_2$  on systemic  
10  
11 386 and cerebral haemodynamics.

12 387  
13  
14 388 Fourthly, estimation of logistic curve parameters is not a straightforward procedure. For the  
15  
16 389 case of expressing the ARI dependence on  $\text{EtCO}_2$  using a sigmoid curve, the problem is  
17  
18 390 worsened by the high variability of ARI estimates, mainly when using a 60 s moving window  
19  
20 391 coupled to an ARMA model (Dineen *et al* 2010). The choice of breaking down each of the six  
21  
22 392 recordings into four data segments of equal duration, aimed to achieve a compromise between  
23  
24 393 obtaining relatively robust mean values over each of these segments, and having enough  
25  
26 394 degrees of freedom ( $6 \times 4 = 24$ ) to be able to estimate the four main parameters of the logistic  
27  
28 395 model. Noteworthy, this was an empirical choice and more work is needed to assess the  
29  
30 396 sensitivity of parameter estimates to other alternatives. We found the combination of least  
31  
32 397 squares with the bootstrap removal of outliers a fairly robust approach to this problem, as  
33  
34 398 shown by the relatively small model errors (Table 2). Nevertheless improvements in this area,  
35  
36 399 and further validation studies, are warranted to achieve new methods for the unsupervised  
37  
38 400 estimation of logistic curve parameters in the presence of low signal-to-noise ratio  
39  
40 401 measurements, as is the case for ARI and CrCP (Panerai 2014).

41  
42 402  
43 403 Importantly, although we have elected to use the ARI index to describe the dependence of dCA  
44  
45 404 on  $\text{PaCO}_2$ , due to its widespread use in the literature, this is by no means the only option.  
46  
47 405 Available and alternative indices, such as TFA phase or the Mx index could be equally  
48  
49 406 employed for this purpose, as long as there are enough data points to describe the logistic curve  
50  
51 407 across the physiological range of  $\text{PaCO}_2$ . Mx is a mean index, based on continuous assessment  
52  
53 408 of slow and spontaneous fluctuations of CBFV and cerebral perfusion pressure offering  
54  
55 409 information on cerebral pressure reactivity (Czosnyka *et al* 1996). With different indices  
56  
57 410 though, it is likely that the scatter of the four parameters describing the logistic model (Table  
58  
59 411 3) would be different, thus affecting future use of these data for calculation of adequate sample  
60  
61 412 sizes.

62  
63 413 Finally, future studies using larger number of subjects, might be able to provide a better  
64  
65 414 characterization of the dependence of the logistic model due to additional co-factors, such as

1  
2  
3 415 aging, posture or autonomic nervous system function. In addition, the lack of consideration for  
4  
5 416 menstrual phase may be considered relevant, however, 36% of female participants were above  
6  
7 417 the age of 50 therefore may have been post-menopausal, suggesting a likely lack of influence  
8  
9 418 on the results.

## 10 11 419 **Conclusions**

12  
13  
14 420 Expressing the influence of PaCO<sub>2</sub> on CBF and its regulatory mechanisms, with a logistic curve  
15  
16 421 reflecting the dependence of ARI as a function of EtCO<sub>2</sub>, represents a new paradigm for the  
17  
18 422 simultaneous assessment of dCA and CO<sub>2</sub> vasoreactivity. This new approach has considerable  
19  
20 423 potential to improve the sensitivity and specificity of dCA assessment in clinical studies of  
21  
22 424 cerebrovascular conditions, but further studies are needed involving older individuals and to  
23  
24 425 establish the reliability of this approach.

## 25 426 **Competing interests**

26  
27  
28 427 No competing interests.

## 29 30 428 **Acknowledgements**

31  
32 429 JSM is a Dunhill Medical Trust Clinical Research Training Fellow (RTF97/0117) at the  
33  
34 430 Department of Cardiovascular Sciences, University of Leicester. TGR is an NIHR Senior  
35  
36 431 Investigator. We thank the subjects for their willingness to participate. This work falls under  
37  
38 432 the portfolio of research conducted within the NIHR Leicester Biomedical Research Centre.

39  
40 433

41  
42  
43  
44  
45  
46  
47  
48  
49  
50  
51  
52  
53  
54  
55  
56  
57  
58  
59  
60

Accepted Manuscript

434 **References**

- 435 Aaslid R, Lindegaard K F, Sorteberg W and Nornes H 1989 Cerebral autoregulation dynamics  
436 in humans *Stroke* **20** 45-52.
- 437 Ainslie P N, Celi L, McGrattan K, Peebles K and Ogoh S 2008 Dynamic cerebral  
438 autoregulation and baroreflex sensitivity during modest and severe step changes in arterial  
439 PCO<sub>2</sub> *Brain Res.* **1230** 115-124.
- 440 Battisti-Charbonney A, Fisher J and Duffin J 2011 The cerebrovascular response to carbon  
441 dioxide in humans *J. Physiol.* **589** 3039-3048.
- 442 Claassen J A, Meel-van den Abeelen A S, Simpson D M, Panerai RB and International Cerebral  
443 Autoregulation Research Network (CARNet) 2016 Transfer function analysis of dynamic  
444 cerebral autoregulation: A white paper from the International Cerebral Autoregulation  
445 Research Network *J. Cereb. Blood Flow Metab.* **36** 665-680.
- 446 Claassen J A, Zhang R, Fu Q, Witkowski S and Levine B D 2007 Transcranial Doppler  
447 estimation of cerebral blood flow and cerebrovascular conductance during modified  
448 rebreathing *J. Appl. Physiol.* **102** 870-877.
- 449 Coverdale N S, Gati J S, Opalevych O, Perrotta A and Shoemaker J K 2014 Cerebral blood  
450 flow velocity underestimates cerebral blood flow during modest hypercapnia and  
451 hypocapnia *J. Appl. Physiol.* **117** 1090-1096.
- 452 Czosnyka, M., Smielewski, P., Kirkpatrick, P., Menon, D.K. & Pickard, J.D. 1996 Monitoring  
453 of cerebral autoregulation in head-injured patients *Stroke* **27** 1829-1834.
- 454 Dineen N E, Brodie F G, Robinson T G and Panerai R B 2010 Continuous estimates of dynamic  
455 cerebral autoregulation during transient hypocapnia and hypercapnia *J. Appl. Physiol.* **108**  
456 604-613.
- 457 Duffin J, Sobczyk O, Crawley A, Poublanc J, Venkatraghavan L, Sam K, Mutch A, Mikulis D  
458 and Fisher J 2017 The role of vascular resistance in BOLD responses to progressive  
459 hypercapnia *Hum. Brain Mapping* **38** 5590-5602.
- 460 Grune F, Kazmaier S, Stolker R J, Visser G H and Weyland A 2015 Carbon dioxide induced  
461 changes in cerebral blood flow and flow velocity: role of cerebrovascular resistance and  
462 effective cerebral perfusion pressure *J. Appl. Physiol.* **35** 1470-1477.
- 463 Ide K, Eliasziw M and Poulin M J 2003 Relationship between middle cerebral artery blood  
464 velocity and end-tidal PCO<sub>2</sub> in the hypocapnic-hypercapnic range in humans *J. Appl.*  
465 *Physiol.* **95** 129-137.
- 466 Kenakin T 1997 *Pharmacologic Analysis of Drug-Receptor Interaction*, 3rd Edition,  
467 Lippincott-Raven, Philadelphia.
- 468 Lassen N A 1959 Cerebral blood flow and oxygen consumption in man *Physiol. Rev.* **39** 183-  
469 238.

- 1  
2  
3 470 Maggio P, Salinet A S, Panerai R B and Robinson T G 2013 Does hypercapnia-induced  
4 471 impairment of cerebral autoregulation affect neurovascular coupling? A functional TCD  
5 472 study. *J. Appl. Physiol.* **115** 491-497.
- 6  
7  
8 473 Markwalder T M, Grolimund P, Seiler R W, Roth F and Aaslid R 1984 Dependency of blood  
9 474 flow velocity in the middle cerebral artery on end-tidal carbon dioxide partial pressure--a  
10 475 transcranial ultrasound Doppler study *J. Appl. Physiol.* **4** 368-372.
- 11  
12 476 McCulloch T J and Turner M J 2009 The effects of hypocapnia and the cerebral autoregulatory  
13 477 response on cerebrovascular resistance and apparent zero flow pressure during isoflurane  
14 478 anesthesia *Anesthesia & Analgesia* **108** 1284-1290.
- 15  
16  
17 479 Minhas J S, Syed N F, Haunton V J, Panerai R B, Robinson T G and Mistri A K 2016 Is  
18 480 dynamic cerebral autoregulation measurement using transcranial Doppler ultrasound  
19 481 reproducible in the presence of high concentration oxygen and carbon dioxide? *Physiol.*  
20 482 *Meas.***37** 673-682.
- 21  
22  
23 483 Ogoh S, Hayashi N, Inagaki M, Ainslie P N and Miyamoto T 2008 Interaction between the  
24 484 ventilatory and cerebrovascular responses to hypo- and hypercapnia at rest and during  
25 485 exercise *J. Physiol.* **586** 4327-4338.
- 26  
27 486 Ogoh S, Nakahara H, Ainslie P N and Miyamoto T 2010 The effect of oxygen on dynamic  
28 487 cerebral autoregulation: critical role of hypocapnia *J. Appl. Physiol.* **108** 538-543.
- 29  
30 488 Panerai R B 2014 Nonstationarity of dynamic cerebral autoregulation *Med. Eng. Physics* **36**  
31 489 576-584.
- 32  
33 490 Panerai R B 2003 The critical closing pressure of the cerebral circulation *Med. Eng. Physics*  
34 491 **25** 621-632.
- 35  
36  
37 492 Panerai R B, Deverson S T, Mahony P, Hayes P and Evans D H 1999 Effects of CO<sub>2</sub> on  
38 493 dynamic cerebral autoregulation measurement *Physiol. Meas.***20** 265-275.
- 39  
40  
41 494 Paulson O B, Strandgaard S and Edvinsson L 1990 Cerebral autoregulation *Cereb. Brain Met.*  
42 495 *Revs.* **2** 161-192.
- 43  
44 496 Poublanc J, Crawley A P, Sobczyk O, Montandon G, Sam K, Mandell D M, Dufort P,  
45 497 Venkatraghavan L, Duffin J, Mikulis D J and Fisher J A 2015 Measuring cerebrovascular  
46 498 reactivity: the dynamic response to a step hypercapnic stimulus *J. Appl. Physiol.* **35** 1746-  
47 499 1756.
- 48  
49  
50 500 Poulin M J, Liang P J and Robbins P A 1996 Dynamics of the cerebral blood flow response to  
51 501 step changes in end-tidal PCO<sub>2</sub> and PO<sub>2</sub> in humans *J. Appl. Physiol.* **81** 1084-1095.
- 52  
53 502 Reivich M 1964 Arterial PCO<sub>2</sub> and Cerebral Hemodynamics *Am. J. Physiol.* **206** 25-35.
- 54  
55 503 Salinet A S, Robinson T G and Panerai R B 2015 Effects of cerebral ischemia on human  
56 504 neurovascular coupling, CO<sub>2</sub> reactivity, and dynamic cerebral autoregulation *J. Appl.*  
57 505 *Physiol.* **118** 170-177.
- 58  
59  
60

- 1  
2  
3 506 Smirl J D, Tzeng Y C, Monteleone B J and Ainslie P N 2014 Influence of cerebrovascular  
4 507 resistance on the dynamic relationship between blood pressure and cerebral blood flow in  
5 508 humans *J. Appl. Physiol.* **12** 1614-1622.
- 7  
8 509 Tiecks F P, Lam A M, Aaslid R and Newell D W 1995 Comparison of static and dynamic  
9 510 cerebral autoregulation measurements *Stroke* **6** 1014-1019.
- 11 511 Tymko M M and Ainslie P N 2017 To regulate, or not to regulate? The devious history of  
12 512 cerebral blood flow control *J. Physiol.* **595**: 5407-5408
- 14  
15 513 Tzeng Y C and Ainslie P N 2014 Blood pressure regulation IX: cerebral autoregulation under  
16 514 blood pressure challenges *Eur. J. App. Physiol.* **114** 545-559.
- 18 515 Verbree J, Bronzwaer A S, Ghariq E, Versluis M J, Daemen M J, van Buchem M A, Dahan A,  
19 516 van Lieshout J J and van Osch M J 2014 Assessment of middle cerebral artery diameter  
20 517 during hypocapnia and hypercapnia in humans using ultra-high-field MRI *J. Appl.*  
21 518 *Physiol.* **117** 1084-1089.
- 23  
24 519 Willie C K, Macleod D B, Shaw A D, Smith K J, Tzeng Y C, Eves N D, Ikeda K, Graham J,  
25 520 Lewis N C, Day T A and Ainslie P N 2012 Regional brain blood flow in man during acute  
26 521 changes in arterial blood gases *J. Physiol.* **590** 3261-3275.
- 28  
29 522 Willie C K, Tzeng Y, Fisher J A and Ainslie P N 2014 Integrative regulation of human brain  
30 523 blood flow *J. Physiol.* **592** 841-859.

31  
32 524  
33  
34  
35  
36  
37  
38  
39  
40  
41  
42  
43  
44  
45  
46  
47  
48  
49  
50  
51  
52  
53  
54  
55  
56  
57  
58  
59  
60

1  
2  
3 **Tables**  
4

5 **Table 1. Population characteristics and baseline parameter values.**  
6

7

8 <b>Parameter</b>	9 <b>All Subjects (n=45)</b>
10 Age (years)	37.5 (14.4)
11 CBFV (cm s <sup>-1</sup> )	57.0 (12.6)
12 Mean ABP (mm Hg)	85.9 (12.4)
13 EtCO <sub>2</sub> (mmHg)	37.8 (3.2)
14 Heart rate (beats/min)	69.4 (11.6)
15 CrCP (mm Hg)	32.1 (12.4)
16 RAP (mmHg cm s <sup>-1</sup> )	1.03 (0.36)
17 Brachial systolic BP (mmHg)	119.1 (17.1)
18 Brachial diastolic BP (mmHg)	70.4 (10.9)
19 ARI	5.5 (1.6)

20 Values are mean (SD). CBFV, cerebral blood velocity; ABP arterial blood pressure; EtCO<sub>2</sub>, end-tidal arterial pressure of carbon dioxide; CrCP, critical closing  
21 pressure; RAP, resistance area product; ARI, Autoregulation Index. CBFV, CrCP, RAP and ARI were averaged for the right and left MCAs.  
22  
23  
24  
25  
26  
27  
28  
29  
30  
31  
32  
33  
34  
35  
36  
37  
38  
39  
40  
41  
42  
43  
44  
45  
46

**Table 2. Population distribution values of logistic model parameters for CBFV, ARI, HR, ABP, CrCP and RAP as a function of EtCO<sub>2</sub>.**

Parameters	CBFV (cm.s <sup>-1</sup> )	ARI	HR (bpm)	ABP (mmHg)	CrCP (mmHg)	RAP (mmHg/cm.s <sup>-1</sup> )
EtCO <sub>2min</sub> (mmHg)	25.9 (5.6)	25.9 (5.6)	25.9 (5.6)	25.9 (5.6)	25.9 (5.6)	25.9 (5.6)
EtCO <sub>2max</sub> (mmHg)	47.9 (3.5)	47.9 (3.5)	47.9 (3.5)	47.9 (3.5)	47.9 (3.5)	47.9 (3.5)
Parameter <sub>min</sub>	41.2 (9.3)	6.9 (1.0)	71.3 (12.3)	79.9 (16.2)	43.4 (16.1)	1.5 (0.5)
Parameter <sub>max</sub>	70.5 (19.2)	2.9 (1.4)	67.6 (11.9)	93.1 (11.4)	23.3 (19.1)	0.8 (0.3)
k coefficient (mmHg <sup>-1</sup> )	0.4 (0.2)	0.3 (0.2)	1.00 (0.8)	0.7 (0.7)	0.4 (0.4)	0.5 (0.6)
x <sub>0</sub> coefficient (mmHg)	36.5 (3.6)	36.5 (4.9)	33.1 (7.1)	34.5 (7.4)	38.4 (4.3)	34.0 (6.8)
MSE (variable units)	1.3 (0.5)	0.7 (0.3)	1.4 (0.8)	2.3 (1.3)	2.8 (1.1)	0.2 (0.1)

Values are mean (SD) (n=45). CBFV, cerebral blood velocity; ABP, arterial blood pressure; EtCO<sub>2min</sub>, minimum values of end-tidal carbon dioxide during hypocapnia; EtCO<sub>2max</sub>, maximum values of end-tidal carbon dioxide during hypercapnia; CrCP, critical closing pressure; RAP, resistance area product; ARI, Autoregulation Index; k coefficient: exponential gain coefficient; x<sub>0</sub> coefficient: EtCO<sub>2</sub> level corresponding to peak derivative of the logistic curve; MSE: mean square error, same units as dependent variables. CBFV, CrCP, RAP and ARI were averaged for the right and left MCAs.

## Figure Legends

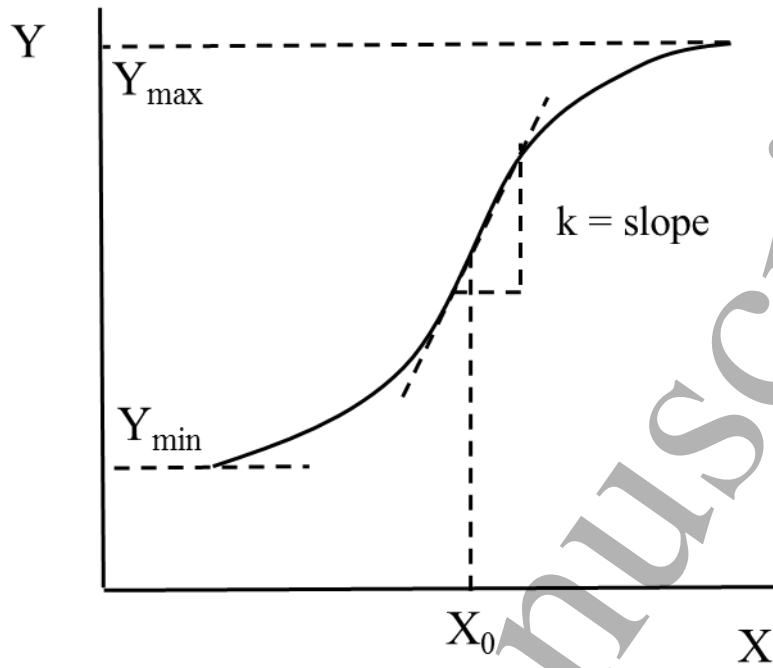
Figure 1. Schematic representation of the four parameter logistic function demonstrating the shape and relationship between parameters.  $y$  can represent either mean CBFV, ABP, HR, CrCP, RAP or ARI;  $x$  is the EtCO<sub>2</sub> level and  $k$  is the exponential gain coefficient. Fitting the model allows estimation of its four parameters, namely  $y_{max}$ ,  $y_{min}$ ,  $k$  and  $x_0$ .

Figure 2. Representative recordings from a 21-year-old female study participant. A. Normocapnia, B. Hypercapnia (8% CO<sub>2</sub>), C. Hypocapnia (-10mmHg from baseline). Dotted vertical lines represent onset of respective manoeuvres.

Figure 3. Logistic model fitting for same subject as in Fig. 1 for (A) CBFV and (B) ARI as a function of EtCO<sub>2</sub>.

Figure 4. Population average logistic model curves for the dependence of (a) CBFV and ARI, (b) HR, ABP, CrCP and RAP. Corresponding shaded areas represent the  $\pm 1$  SEM boundaries.

Accepted Manuscript



Accepted Manuscript

